Electron Spin Echo Envelope Modulation (ESEEM) Spectroscopy of Cobalt(II) Bis(dimethylglyoximes): Equatorial Co–N Coupling Parameters

Michael D. Wirt,*,† Christopher J. Bender,† and Jack Peisach†,‡

Departments of Molecular Pharmacology and Physiology and Biophysics, Albert Einstein College of Medicine, Yeshiva University, Bronx, New York 10461

Received May 13, 1994[⊗]

We present the first direct measurement of Co–N(equatorial) coupling parameters, obtained from electron spin echo envelope modulation (ESEEM) spectroscopy, of *trans*-bis(dimethylglyoximato)bis(methanol)- and -bis(pyridine)cobalt(II) species. ESEEM spectroscopy provides a means to detect changes in unpaired spin density in the equatorial plane. Simulation of Fourier transformed ESEEM spectra of the low-spin cobalt(II) dimethylglyoxime complexes, collected in frozen methanol/toluene solution, reveal coupling parameters from four nearly magnetically equivalent, equatorially coordinated ^{14}N nuclei. Modulation of Co–N(equatorial) coupling is observed when the σ-bonding strength of the axial ligands is increased from weakly coordinated methanol solvent to the more strongly coordinated bis(pyridine) complex. Nuclear hyperfine and quadrupole coupling parameters for the bis(methanol) and bis(pyridine) species are as follows: $A_{iso} = 2.1 \pm 0.1$ MHz, $e^2qQ = 3.40 \pm 0.05$ MHz; and $A_{iso} = 1.17 \pm 0.05$ MHz, $e_2qQ = 3.40 \pm 0.05$ MHz, respectively. Reduction in the magnitude of Co–N(equatorial) coupling for the dimethylglyoxime species is consistent with a decrease in unpaired spin density on cobalt upon coordination of pyridine. Localization of the principle axis of the nuclear quadrupole interaction within the cobalt(II) bis(dimethylglyoxime) plane (Euler angle β = ca. 95°) emphasizes the magnetic differences between dimethylglyoximes and porphine systems where the value for β is consistently reported near 45° (Magliozzo, R. S.; Peisach, J. *Biochemistry*, **1993**, *33*, 8446).

Introduction

For several years, *trans*-bis(dimethylglyoximato)cobalt complexes have been extensively studied as cobalamin models.[1–6] These complexes contain two singly-deprotonated dioxime ligands that are hydrogen bonded to each other (resulting in a four nitrogen donor ring system that is approximately coplanar).[5,6] The two remaining axial sites can be occupied to complete an octahedral geometry (Figure 1).

Continuous-wave electron paramagnetic resonance (CW-EPR) and electron–nuclear double resonance (ENDOR) studies of low-spin cobalt(II) corrinoids and cobalt(II) bis(dimethylglyoxime) (dmg) compounds have established trends in nuclear hyperfine coupling constants for several axial ligand combinations.[7–11] Localization of the magnetization in the d_z^2 orbital (perpendicular to the dmg and corrin ring planes) provides a means to detect changes in axial ligation, but significantly reduces our ability to determine in-plane (equatorial) coupling parameters by conventional CW-EPR methods.

Electron spin echo envelope modulation (ESEEM) spectroscopy provides a unique method for determination of weak superhyperfine coupling constants in paramagnetic biomolecules.[12,13] Analysis of ESEEM data permits not only determination of magnetic coupling parameters and numbers of nuclei contributing to the ESEEM but also the relative orientations of their crystallographic, **g**, and hyperfine tensors (axis) with respect to the paramagnetic center.[14,15]

We present the first direct measure of Co–N equatorial (eq) coupling parameters, obtained from ESEEM spectroscopy, of cobalt(II) *trans*-bis(dimethylglyoximate) bis(methanol) ($Co^{II}(dmg)_2(CH_3OH)_2$) and bis(pyridine) ($Co^{II}(dmg)_2(py)_2$) species (Table 1). Simulation of Fourier transformed ESEEM spectra of Co(II)–dmg complexes reveal coupling parameters from four nearly magnetically equivalent, equatorially coordinated ^{14}N nuclei.

Experimental Section

Materials. Dimethylglyoxime (98%) was obtained from Eastman Organic Chemicals. [^{14}N]Pyridine (99.9%) was obtained from Aldrich Chemical Co. [^{15}N]Pyridine(99%) was obtained from ICON Services Inc. Co(II) acetate tetrahydrate was purchased from Alfa Products. All were used without further purification.

* To whom correspondence should be addressed.
† Department of Molecular Pharmacology.
‡ Department of Physiology and Biophysics.
⊗ Abstract published in *Advance ACS Abstracts*, March 1, 1995.

(1) Glusker, J. P. In B_{12}; Dolphin, D., Ed.; J. Wiley & Sons: New York, 1982; Vol. 1, pp 23–106.
(2) Toscano, P. J.; Marzilli, L. G. *Prog. Inorg. Chem.* **1984**, *31*, 105.
(3) Schrauzer, G. N. *Acc. Chem. Res.* **1968**, *1*, 97.
(4) Dolphin, D. In B_{12}; Dolphin, D., Ed.; J. Wiley & Sons: New York, 1982; Vols. **1** and **2**.
(5) Bresciani-Pahor, N.; Forcolin, M.; Marzilli, L. G.; Randaccio, L.; Summers, M. F.; Toscano, P. *J. Coord. Chem. Rev.* **1985**, *63*, 1.
(6) Fallon, G. D.; Gatehouse, B. M. *Cryst. Struct. Commun.* **1978**, *7*, 263.
(7) Rockenbauer, A.; Bodo-Zahonyi, E.; Simandi, L. I. *J. Chem. Soc. Dalton Trans.* **1975**, 1729.
(8) Bayston, J. H.; Looney, F. D.; Pilbrow, J. R.; Winfield, M. E. *Biochemistry* **1970**, *9*, 216.
(9) Jorin, E.; Schweiger, A.; Gunthard, Hs. H. *J. Am. Chem. Soc.* **1983**, *105*, 4277.
(10) Schweiger, A.; Jorin, E.; Gunthard, Hs. H. *Chem. Phys. Lett.* **1979**, *61*, 223.
(11) Baumgarten, M.; Lubitz, W.; Winscom, C. J. *Chem. Phys. Lett.* **1987**, *133*, 102.
(12) Mims, W. B.; Peisach, J. In *Biological Applications of Magnetic Resonance*; Schulman, R. G., Ed.; Academic Press: New York, 1979; pp 221–269.
(13) Mims, W. B.; Peisach, J. In *Advanced EPR, Applications in Biology and Biochemistry*; Hoff, A. J., Ed.; Elsevier: Amsterdam, 1989; pp 1–57.
(14) Mims, W. B. *Phys. Rev. B* **1972**, *5*, 2409.
(15) McCracken, J.; Cornelius, J. B.; Peisach, J. In *Pulsed EPR: A New Field of Applications*; Keitjers, C. P., Reijerse, E. J., Schmidt, J., Eds.; North Holland: Amsterdam, 1989; p 156.

0020-1669/95/1334-1663$09.00/0

Table 1. ESEEM Simulation Parameters for $Co^{II}(dmg)_2(CH_3OH)_2$ and $Co^{II}(dmg)_2(^{15}N(py)_2)^a$

compound	e^2Qq (MHz)	η	θ_N (deg)	ϕ_N (deg)	α (deg)	β (deg)	γ (deg)	r_{eff} (Å)	A_{iso} (MHz)
$Co^{II}(dmg)_2(CH_3OH)_2$	3.4	0.70	95.4	3.0	1.9	98.0	15.0	3.1	2.10
$Co^{II}(dmg)_2(^{15}N(py)_2)$	3.4	0.70	95.0	8.0	6.3	96.0	5.0	2.9	1.17

[a] Experimental parameters included in the simulation are specified in Figure 2. Variable parameters that are refined to describe the nuclear quadrupole and hyperfine tensors include the nitrogen nuclear quadrupole coupling parameter, e^2qQ, and the quadrupole interaction asymmetry parameter, η, which describe the magnitude and symmetry of the nuclear quadrupole tensor, and Euler angles, α, β, and γ which relate rotations needed to allign the principle axis of the quadrupole tensor to those of the **g** tensor. The nuclear hyperfine tensor is described by A_{iso}, the isotropic nuclear hyperfine coupling constant, r_{eff}, an effective dipole−dipole distance, and two angles, θ_N and ϕ_N, which relate the relative orientations of the nuclear hyperfine tensor to the **g** tensor. Simulations are conducted by refining individual variable parameters while holding others fixed until simultaneous fits are obtained for experimental data collected at several g values.

Table 2. Comparison of CW-EPR and ENDOR Results for Selected Cobalt(II) Dimethylglyoxime and Cobalt(II) Porphyrin Complexes[a]

complex	CN	$g_\perp$	$g_\parallel$	$A_\perp^{Co}$ (G)	$A_\parallel^{Co}$ (G)	$A_\parallel^{N}$ (G)	solvent	method
$Co^{II}(dmg)_2$[a]	6	2.236	2.0106	28.6	102.0		methanol	CW-EPR[7]
$Co^{II}(dmg)_2(py)$	5	2.24	2.0137	15.0	86.5	15.5	methanol/py	CW-EPR[7]
$Co^{II}(dmg)_2(py)_2$	6	2.205	2.0161	15.8	78.0	15.8	methanol/py	CW-EPR[7]
$Co^{II}(p\text{-}OCH_3)TPP$[c]	4	2.848	2.006	228.0	161.0		toluene	CW-EPR[29]
$Co^{II}(p\text{-}OCH_3)TPP(py)$[c]	5	≥2.327[b]	2.025	≤12[b]	79.8	15.6	toluene/py	CW-EPR[29]
$Co^{II}(p\text{-}OCH_3)TPP(py)_2$[c]	6	2.216	2.047	57.0	60.0	11.2	toluene/py	CW-EPR[29]
$Co^{II}(dmg)_2(py)_2$[d]	6	$x = 2.270$ $y = 2.137$	2.018	$x = 6.3$ $y = 5.7$	90.9	15.6	methanol/py	ENDOR[18]
$Co^{II}OEP(py)$[e]	5	$x = 2.329$ $y = 2.326$	2.025	$x = 7.1$ $y = 8.0$	82.6	15.3 (^{14}N) 21.5 (^{15}N)	chloroform/py	ENDOR[18]

[a] Bis(dimethylglyoxime) (dmg); axial water molecules have been replaced by weakly coordinated methanol solvent in the Co(II)$(dmg)_2$ species.[17] [b] Cobalt hyperfine coupling unresolved; estimates based on total line width, or not reported. [c] (p-OCH_3)TPP = tetra(methoxyphenyl)porphyrin. [d] ENDOR data collected by Baumgarten and Lubitz[11] are in good agreement with the results of Greiner *et al.*[18] [e] OEP = octaethylporphine.

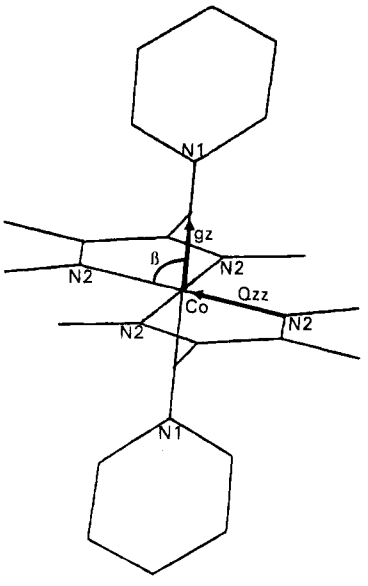

Figure 1. Structure of the *trans*-bis(dimethylglyoximato)bis(pyridine)-cobalt(II) complex. The axial sites are quite flexible and can be occupied by various combinations of neutral and anionic ligands.[5] The direction of g_z lies along the Co−axial bond, perpendicular to the equatorial plane.[11,35] The nuclear quadrupole interaction tensor $\mathbf{Q}_{zz}$ lies coincident with the Co−N(eq) bond. The Euler rotation angle, β describes the angle between g_z and $\mathbf{Q}_{zz}$. The structure was obtained from the Cambridge Crystallographic Data Base (version 5).[37] Hydrogen atoms have been removed from the structure for clairity.

Sample Preparation. *trans*-Bis(dimethylglyoximato)bis-(aquo)cobalt(II)[16] and *trans*-bis(dimethylglyoximato)bis(pyridine)cobalt(II)[7] were prepared by standard methods under argon. $Co^{II}(dmg)_2(CH_3OH)_2$ EPR samples were prepared by degassing a 50/50 (v/v) methanol/toluene solution in a quartz EPR tube. Crystalline $Co^{II}(dmg)_2(H_2O)_2$ was subsequently added to the degassed solvent, under argon, and the EPR tube was immediately plunged into liquid nitrogen and sealed. Previous stability constant experiments of Rockenbauer *et al.*[17] show that the water ligands of the diaquo complex are replaced by weakly coordinated methanol upon solvation. $Co^{II}(dmg)_2((^{14}N)py)_2$ and $Co^{II}(dmg)_2((^{15}N)py)_2$ were prepared by adding a **2:1** molar ratio of ^{14}N or ^{15}N pyridine to the methanol/toluene solution prior to the addition of crystalline $Co^{II}(dmg)_2(H_2O)_2$. The EPR tubes containing the bis(pyridine) complex were submerged in liquid nitrogen and sealed under argon. Cobalt(II) bis(dimethylglyoxime) samples were prepared to a final concentration of ca. 5 mM. The methanol/toluene solvent system provided a good glass for collecting ESEEM data at 4.2 K.

EPR Spectroscopy. Co(II) dmg samples were characterized by X-band CW-EPR at 77 K using a Varian E112 spectrometer. $g_\parallel$, $g_\perp$ and $A_\parallel^{Co}$ values for the $Co^{II}(dmg)_2(CH_3OH)_2$ species (estimated from CW-EPR spectra) are 2.009, 2.240 and 106 G, respectively. For the $Co^{II}(dmg)_2(^{14}N(py))_2$ complex, $g_\parallel = 2.024$ and $g_\perp = 2.254$, with $A_\parallel^{Co} = 84$ G and $A^N = 15.8$ G. The bis($[^{14}N]$pyridine) spectra contained the expected 1:2:3:2:1 superhyperfine pattern consistent with two pyridine ligands axially coordinated to cobalt. $Co^{II}(dmg)_2(^{15}N(py))_2$ had values of $g_\parallel = 2.024$, $g_\perp = 2.254$, $A_\parallel^{Co} = 84$ G, and $A^N = 22.2$ G and contained a three-line superhyperfine structure for two axially coordinated ^{15}N nuclei. Both $g_\parallel$ and $g_\perp$ as well as $A_\parallel$ values for the Co(II)−dmg compounds are consistent with those of Rockenbauer *et al.*[7] and Greiner *et al.*[11,18] (Table 2).

ESEEM spectra were collected at 4.2 K using a pulsed EPR spectrometer[19] equipped with a folded strip-line microwave cavity[20] using a stimulated echo (90° $-\tau-$90°$-T-$90°) pulse

(16) Schrauzer, G. N. In *Methods in Inorganic Chemistry*; Jolly, W. L., Ed.; McGraw-Hill: New York, 1968; Vol. 11, pp 61−69.
(17) Rockenbauer, A.; Budo-Zahonyi, E.; Simandi, L. I. *J. Coord. Chem.* **1972**, *2*, 53.
(18) Greiner, S. P.; Baumgarten, M. *J. Magn. Reson.* **1989**, *83*, 630.
(19) McCracken, J.; Peisach, J.; Dooley, D. M. *J. Am. Chem. Soc.* **1987**, *109*, 4064.

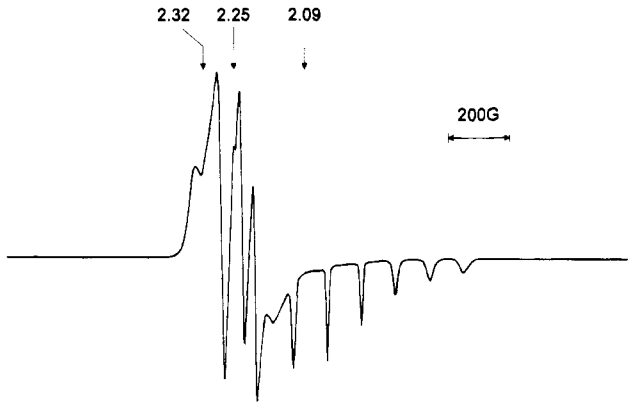

Figure 2. X-Band EPR spectrum of $Co^{II}(dmg)_2(CH_3OH)_2$. Samples were prepared as 5 mM frozen solutions in methanol−toluene (1:1). The three arrows indicate the field positions at which the ESEEM spectra were collected. Experimental conditions: temperature = 77 K, field modulation = 100 kHz, modulation amplitude = 10 G, microwave power = 5.0 mW, microwave frequency = 9.231 GHz.

sequence.[21] The delay between the first and second microwave pulses, τ, was set to multiples of the proton Zeeman frequency in order to suppress modulation by weakly coupled protons.[21] The time dependent echo modulation was Fourier transformed into the frequency domain and data lost to instrumental dead time was reconstructed by the methods of Mims.[22] Co(II)−dmg spectra were collected at three different magnetic field settings (g_{max}, g_{mid}, and g_{min}) within the EPR absorption for each complex (Figure 2). Collection of ESEEM data at these positions within the EPR absorption often gives single-crystal-like ENDOR/ESEEM spectra.[23]

Spectral Simulations. ESEEM data analysis was completed by simulation of the experimental data, acquired at each magnetic field setting, by both manual and nonlinear least-squares techniques. The basis of these simulations is the perturbational spin hamiltonian and the density matrix formalism of Mims[14] Simulation of powder ESEEM spectra requires a complete set of nuclear hyperfine parameters for both the central metal ion and the interacting nitrogen atoms. The g-axis is the reference frame, and Euler angles α, β, and γ are specified for the principal axis of the metal hyperfine, nitrogen hyperfine and nitrogen quadrupole tensors. Cobalt hyperfine g_x, g_y and g_z values were obtained from previous simulations of CW-EPR[7] ($Co^{II}(dmg)_2$) and ENDOR[18] ($Co^{II}(dmg)_2(py)_2$ data (Table 2). ESEEM simulations for the bis(pyridine) complex were conducted using g and cobalt hyperfine parameters from both CW-EPR[7] and ENDOR[18] experiments as a test. Differences in fitting results obtained from the two sources are within the error of the equatorial couplings. The fitting process entails optimization of the simulated solution by manually varying the nitrogen hyperfine and quadrupole parameters and their tensor orientations.

A recent improvement to the manual simulation program is the adoption of a nonlinear least-squares (sum of the residuals squared, χ^2) method to fit modulation patterns for ESEEM data in the time domain. Simulated spectra obtained by the nonlinear least-squares (Levenberg−Marquardt[24,25]) method can be Fourier transformed to allow for direct comparison of fits obtained by both programs in frequency domain. For an initial set of nine

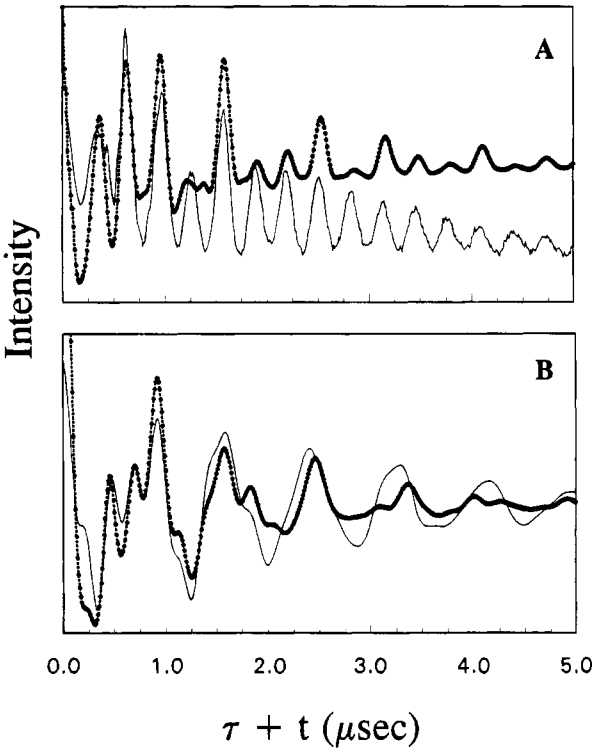

Figure 3. Time−domain ESEEM data (—) and the corresponding simulation (- -) for (A) $Co^{II}(dmg)_2(CH_3OH)_2$ and (B) $Co^{II}(dmg)_2(py)_2$. For the bis(pyridine) complex, ^{15}N pyridine was used as the axial ligand to eliminate possible ambiguous contributions of the $Co-^{14}N(eq)$ couplings to the ESEEM spectrum. Experimental conditions for the bis(methanol) species were as follows: microwave frequency = 8.732 GHz at 3153 G (g_{min}) magnetic field strength, τ = 285 ns. For the bis(pyridine) species: microwave frequency was 8.776 GHz at 3140 G (g_{min}) magnetic field strength, τ = 225 ns. All scans were collected using a 100 Hz repetition rate at 4.2 K.

variable parameters, the program automatically refines the solution to a user defined convergence criterion (*i.e.*, a minimum improvement in χ^2) using an iterative process. Program input parameters are identical to the manual fitting program. All parameters can be varied in any combination during least-squares refinement. Examination of χ^2 values as well as eliminating potential solutions that are not chemically reasonable provides a means to evaluate simulated solutions.

Best fits obtained from the manual and least-squares methods were in good agreement. Comparison of the two methods showed deviations ranging between 5 and 10° for angles and between 0.0 and 0.1 Å for r_{eff}, and were within the reported error for e^2Qq and A_{iso} (Table 1).

Results and Discussion

Co(II)−dmg timg domain spectra and their respective simulations are shown in Figure 3. Strong nitrogen modulations of the electron spin echo (ESE) are observed for both the bis(methanol) and bis(pyridine) species. Nitrogen modulation of the ESE result from both electron−nuclear and nuclear quadrupole interactions between the unpaired electron spin on Co(II) and the directly coordinated equatorial nitrogen nuclei. Axial nitrogen superhyperfine coupling in the bis(pyridine) complex is too large to give rise to envelope modulation.[7,11,26,27]

(20) Britt, R. D.; Klein, M. P. *J. Magn. Reson.* **1987**, *74*, 535.
(21) Mims, W. B.; Peisach, J. In *Biological Magnetic Resonance*; Berliner, L. J., Reuben, J., Eds.; Plenum Press: New York, 1981; Vol. 3, pp 213−263.
(22) Mims, W. B. *J. Magn. Reson.* **1984**, *59*, 291.
(23) Rist, G. H.; Hyde, J. S. *J. Chem. Phys.* **1970**, *52*, 4633.
(24) Marquardt, D. W. *J. Soc. Ind. Appl. Math.* **1963**, *11*, 431.
(25) Press, W. H.; Flannery, B. P.; Teukolsky, S. A.; Vetterling, W. T. In *Numerical Recipes: The Art of Scientific Computing*; Cambridge University Press: Cambridge, England, 1986; pp 1−818.
(26) Cornelius, J. B.; McCracken, J.; Clarkson, R. B.; Belford, R. L.; Peisach, J. *J. Chem. Phys.* **1990**, *94*, 6977.
(27) Mims, W. B.; Peisach, J. *J. Chem. Phys.* **1978**, *19*, 4921.

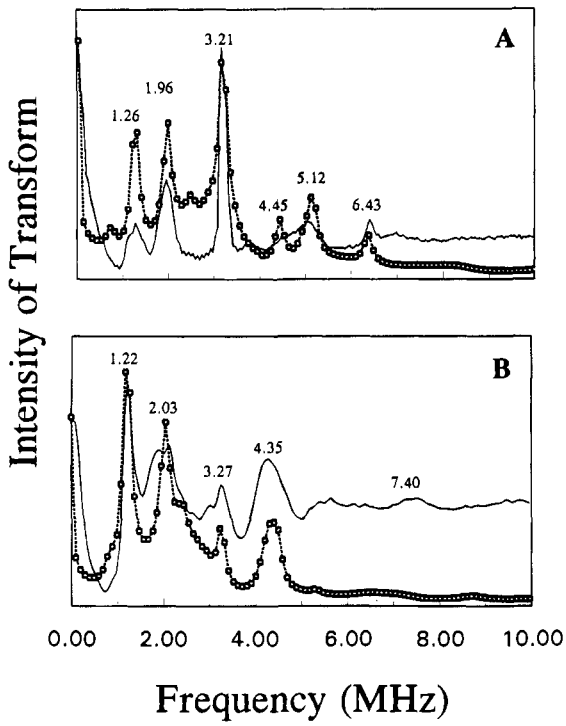

Figure 4. Fourier transform of ESEEM data seen in Figure 3 (—) and the corresponding simulation (- -) for (A) $Co^{II}(dmg)_2(CH_3OH)_2$ and (B) of $Co^{II}(dmg)_2(^{15}N(py)_2)$.

This was verified by collecting ESEEM spectra of both bis([^{14}N]pyridine) and bis([^{15}N]pyridine)cobalt(II)−dmg preparations at g_{mid} (2925 G). No differences were observed.

Fourier transforms of ESEEM data presented in Figure 3 are shown in Figure 4. Both sets of spectra are characteristic of a low-spin $S = {}^1/_2$ (d^7) system coupled to an $I = 1$ nucleus under nearly "exact cancellation" conditions,[28] under which the nuclear Zeeman interaction is equal to approximately half the electron−nuclear coupling. Thus, for one of the ^{14}N spin manifolds, the two terms almost cancel, leaving the nuclear quadrupole interaction to solely determine the energy level splitting. Under these conditions, the resulting ESEEM spectrum contains three distinct quadrupole lines, the frequencies and intensities of which are related to e^2qQ, the quadrupole coupling parameter, η, the asymmetry parameter, and the Euler angles α, β, and γ, respectively.[26] The second spin manifold gives rise to a single broad "double quantum" line corresponding to a $\Delta m_I = 2$ transition, and contains contributions from the nuclear hyperfine term fo the Hamiltonian. In Figure 4a (solid line), the $Co^{II}(dmg)_2(CH_3OH)_2$ spectrum shows sharp quadrupole lines at 1.26, 1.96, and 3.21 MHz. The double quantum line appears at 5.12 MHz. The expected combination bands, due to multiple nitrogen contributions to the ESEEM,[15] appear as a shoulder (4.45 MHz) on the 5.12 MHz line and as a low intensity peak at 6.4 MHz. Spectral simulations conducted at 2835 G (g_{max}), 2925 G (g_{mid}), and 3153 G (g_{min}) magnetic field and several values of τ, gave nuclear hyperfine and quadrupole coupling parameters of $A_{iso} = 2.1 \pm 0.1$ MHZ, $e^2qQ = 3.40 \pm 0.05$ MHz (Figure 4a (dashed line) and Table 1). For the $Co^{II}(dmg)_2(N^{15}(py)_2)$ complex, five lines are observed in the spectrum (Figure 4b (solid line)). Three quadrupole lines are seen at 1.22, 2.03 (midpoint), and 3.27 MHz. The double quantum appears at 4.35 MHz, and a broad low intensity line is observed at 7.4 MHz that may be attributed to a proton interaction. The 7.4 MHz line intensity is quickly reduced with increasing values of τ (from τ = 160 ns to τ = 450 ns) while the four other line intensities remain relatively constant to ca. τ = 300 ns, after which the signal intensity diminishes. When comparing the bis(pyridine) complex to the bis(methanol) dmg, the strength of the quadrupole coupling parameter ($e^2qQ = 3.40 \pm 0.05$ MHz) and the asymmetry parameter ($\eta = 0.70 \pm 0.05$) are unchanged (Table 1). This is not surprising since equatorial nitrogen coordination distances for dmgs are somewhat insensitive to changes in axial ligation.[5] However, the magnitude of A_{iso}, determined by simulation of the $Co^{II}(dmg)_2(py)_2$ data at 2900 G (g_{max}), 2943 G (g_{mid}) and 3140 G (g_{min}) (Figure 4b (dashed line)), decreases to 1.17 ± 0.05 MHz as unpaired spin density is removed from cobalt to the axial pyridines. This trend is consistent with previous CW-EPR work of Rockenbauer *et. al.*,[7] who observed a reduction in the value of the parallel component of the cobalt hyperfine coupling constant ($A_{||}^{Co}$) from 102.0 to 86.5 to 78.0 G for the $Co^{II}(dmg)_2$, $Co^{II}(dmg)_2(py)$, and $Co^{II}(dmg)_2(py)_2$ species, respectively (Table 2). A similar trend for $A_{||}^{Co}$ is observed for CW-EPR and ENDOR data of low-spin Co(II) porphine complexes[29] (Table 2).

Comparison of average Co-N(eq) coupling parameters obtained by ESEEM spectroscopy for low-spin (d^5) myoglobin complexes containing either azide, cyanide, mercaptoethanol or hydroxide as a sixth ligand,[30,31] with low-spin (d^7) Co(II)−dmg Co−N(eq) couplings (Table 1) show differences in both magnitude and number of unique contributions to the equatorial metal-nitrogen coupling. For the Co(II) dmg complexes, the Co−N(eq) coupling is much weaker than that seen for low-spin iron porphines, where Fe−N(eq) couplings are reported in the range of 4−6 MHz.[30,31] Examination of the double quantum transitions at 5.12 and 4.35 MHz for the $Co^{II}(dmg)_2(CH_3OH)_2$ and $Co^{II}(dmg)_2(py)$ species (Figure 4a,b) show no evidence of structure within the peaks, indicating that the coupling arises from four nearly magnetically equivalent equatorial nitrogens. This is not the case for the low-spin iron porphine complexes mentioned previously, where ESEEM spectra for each of these compounds exhibit structure in the double quantum transition that facilitates identification of three magnetically unequal contributions to the Fe−N(eq) couplings.[30,31] In addition, single crystal ENDOR analysis of aquometmyoglobin[32] and Cu(II) and Ag(II) tetraphenylporphine[33] (TPP) have identified unequal equatorial metal−nitrogen couplings from all four porphine pyrrole groups. It is important to note that the four equatorial nitrogens may be symmetry equivalent but magnetically unequal since spin density can be correlated with orbital overlap; therefore, we can use magnetic parameters as an indicator measure for chemical inequivalence.

The origin of the differences between porphine and dmg couplings is not entirely clear. In addition to the obvious structural differences between pyrrole and glyoxime nitrogens and the presence of conjugation in the porphines, a comparison of nitrogen hyperfine coupling parameters for $Co^{II}(dmg)_2(py)_2$ ($A_{||}^N = 15.8$ G)[7] and cobalt(II) tetrakis(methoxyphenyl)porphine bis(pyridine) complex ($A_{||}^N = 11.2$ G)[29] demonstrates a greater degree of unpaired spin density on the axial pyridine nitrogens of the $Co^{II}(dmg)_2(py)_2$ compound (Table 2). Increased spin density on the axial pyridine nitrogens may reduce unpaired spin density in the equatorial dmg plane and provide a partial explanation for the weak equatorial coupling observed in the bis(pyridine) complex. Additionally, the origin of the unpaired

(28) Flanagan, H. L.; Singel, D. J. *J. Chem. Phys.* **1987**, *87*, 5606.
(29) Walker, F. A. *J. Am. Chem. Soc.* **1970**, *92*, 4235.
(30) Magliozzo, R. S.; Peisach, J. *Biochemistry*, **1992**, *31*, 189.
(31) Magliozzo, R. S.; Peisach, J. *Biochemistry*, **1993**, *33*, 8446.
(32) Scholes, C. P.; Lapidot, A.; Mascarenhas, R.; Inubushi, T.; Isaacson, R. S.; Feher, G. *J. Am. Chem. Soc.* **1982**, *104*, 2724.
(33) Brown, T. G.; Hoffman, B. M. *Mol. Phys.* **1980**, *39*, 1073.

spin, derived from the d_{z^2} orbital of the d^7 Co(II)−dmg species[3] and the d_{yz} orbital of the d^5 iron(III) porphine[34] may also contribute to the observed differences due to the potential for π-interactions between the half-filled iron d_{yz} orbital and porphine and/or proximal imidazole nitrogen ligands.[30]

The principle direction of the **g** tensors for both dmg complexes have been determined from previous ENDOR experiments[11,35] and correspond closely with the symmetry axis of the octahedral molecules. The crystal structure of the $Co^{II}(dmg)_2(py)_2$ shows an elongated octahedron with average Co−N(eq) bond distances of 1.89 Å and symmetric Co−N(ax) distances of 2.25 Å.[6] The axial pyridine ligands form approximately 90° angles with a plane containing the four equatorial nitrogen ligands and cobalt (Figure 1). We have assigned g_z to lie along the Co-axial ligand bond and assume g_x and g_y to lie perpendicular to g_z in the dmg plane, consistent with previous ENDOR studies.[11,35] For both complexes, values for θ and ϕ (that relate the relative orientation of the nuclear hyperfine tensor to the **g** tensor) are near 90° and 0°, which orients the electron−nuclear coupling within the dmg plane. Additionally, we have assumed the lone pair donor orbital of the glyoxime nitrogen to be localized within the plane containing the four equatorial dmg nitrogen ligands and cobalt. This assignment is consistent with previous nuclear quadrupole resonance studies of Hsieh *et al.*, for both nickel(II) and palladium(II) bis(dimethylglyoxime) complexes, where the principle axis of the nuclear quadrupole interaction (Q_{zz}) is assigned within the plane of atoms about nitrogen directed toward the coordinating metal.[36] The angle between Q_{zz} and g_z (Figure 1) is described by the Euler rotation angle β, which is determined to be 98° ± 5 and 96° ± 5° for the $Co^{II}(dmg)_2(CH_3OH)_2$ and $Co^{II}(dmg)_2(py)_2$ species respectively. Thus, it is reasonable to suggest that the largest component of the electric field gradient lies along the Co−N σ-bond in the equatorial dmg plane. This result is in contrast to what is seen for the low-spin iron prophine complexes, discussed previously[30,31] as well as for Cu^{II}- and $Ag^{II}TPP$,[32] where values for β are reported near 45° in all cases. Simulations for both dmg complexes, where β was fixed at 45° while refining the remaining parameters, gave a best fit that deviated significantly from the experimental data. The difference in values for β may result from the presence of an "anomalous" nuclear quadrupole axis system for the porphine pyrrole nitrogens, where Q_{zz} is no longer coincident with the lone pair nitrogen donor orbitals.[28,30,33]

Conclusions

Application of the ESEEM technique to study $Co^{II}(dmg)_2(CH_3OH)_2$ and $Co^{II}(dmg)_2(py)_2$ complexes provides an ideal approach to evaluate our ability to measure previously inaccessible Co−N(eq) coupling parameters for this class of compounds. Modulation of Co−N(eq) coupling is observed when the σ-bonding strength of the axial ligands is increased from weakly coordinated methanol solvent to the more strongly coordinated bis(pyridine) complex. Reduction in the magnitude of Co−N(eq) coupling for the dmg species is consistent with a loss of unpaired spin density on cobalt upon coordination of pyridine. Localization of the principle axis of the nuclear quadrupole interaction within the dmg plane (β = ca. 95°) emphasizes the magnetic differences between dmg and porphine systems where the value for β is consistently reported near 45°.[30−33]

Extension of these preliminary ESEEM studies of Co(II)−bis(dmg)s to cobalt(II) cobalamins and enzyme- bound Co(II) cofactors will provide unique insight into magnetic properties of the corrin ring as well as information regarding the orientation of the dimethylbenzimidazole base (arising from remote coupling of the noncoordinated benzimidazole nitrogen[15]) that may influence Co−C bond reactivity upon formation of B_{12} holoenzymes.

Acknowledgment. We would like to thank Drs. Yury Levitansky and Alan Coffino for adaptation of the nonlinear least-squres simulation procedures to our IRIS computer system and Dr. Eric Hustedt for the original nonlinear least-squares FORTRAN code. We would also like to thank Drs. Richard Magliozzo and Caroline Lee for helpful discussions and Eva Scheuring for computer graphics assistance. This research is supported by NIH Grants RR-02583 and GM40168 (J.P.).

IC940539W

(34) Gibson, S. F.; Ingram, D. S. E.; Schunland, D. *Discussions Faraday Soc.* **1958**, *26*, 72.
(35) Nishida, Y.; Kida, S. *Coord. Chem. Rev.* **1979**, *27*, 275.
(36) Hsieh, Y. N.; Ireland, P. S.; Brown, T. L. *J. Magn. Reson.* **1976**, *21*, 445.
(37) Allen, F. H.; Kennard, O.; Taylor, R. *Acc. Chem. Res.* **1983**, *16*, 146.